New Journal of Physics
The open access journal at the forefront of physics
Deutsche Physikalische Gesellschaft DPG | IOP Institute of Physics

Thermal instability of cell nuclei

Enrico Warmt[1], Tobias R Kießling[1], Roland Stange, Anatol W Fritsch, Mareike Zink and Josef A Käs
Institut für Experimentelle Physik I, Universität Leipzig, Leipzig, Germany
E-mail: enrico.warmt@uni-leipzig.de

Received 3 March 2014, revised 14 May 2014
Accepted for publication 21 May 2014
Published 4 July 2014
New Journal of Physics **16** (2014) 073009
doi:10.1088/1367-2630/16/7/073009

Abstract
DNA is known to be a mechanically and thermally stable structure. In its double stranded form it is densely packed within the cell nucleus and is thermo-resistant up to 70 °C. In contrast, we found a sudden loss of cell nuclei integrity at relatively moderate temperatures ranging from 45 to 55 °C. In our study, suspended cells held in an optical double beam trap were heated under controlled conditions while monitoring the nuclear shape. At specific critical temperatures, an irreversible sudden shape transition of the nuclei was observed. These temperature induced transitions differ in abundance and intensity for various normal and cancerous epithelial breast cells, which clearly characterizes different cell types. Our results show that temperatures slightly higher than physiological conditions are able to induce instabilities of nuclear structures, eventually leading to cell death. This is a surprising finding since recent thermorheological cell studies have shown that cells have a lower viscosity and are thus more deformable upon temperature increase. Since the nucleus is tightly coupled to the outer cell shape via the cytoskeleton, the force propagation of nuclear reshaping to the cell membrane was investigated in combination with the application of cytoskeletal drugs.

S Online supplementary data available from stacks.iop.org/njp/16/073009/mmedia

[1] EW and TRK contributed equally to this work.

Keywords: temperature, thermorheology, cell nucleus, optical stretcher, cytoskeleton

1. Introduction

In eukaryotic cells the nucleus is the largest organelle. For instance, the nuclei of suspended cells can occupy about half of the volume of entire cells (see figure 1). The nucleus is not just an unstructured compartment densely packed with DNA. Its spatial organization is quintessential for the transcription of DNA to RNA, as well as translation during the process of gene expression [1].

Within cells, the nuclei are the stiffest cell compartment (2 to 10 times stiffer than the surrounding cytoplasm) [2, 3]. A key structural element is the nuclear lamina, which is a complex 2D intermediate filament meshwork connecting the nuclear envelope to the nuclear interior, as well as the nuclear matrix network branching throughout the inner DNA filled nucleus [4]. Further important organizing proteins are histones [5, 6], which are mainly responsible for packing DNA into compact chromosomes and regulating gene expression. Moreover, physical properties, such as the mechanical stability of the nucleus, contribute strongly to cell fate and survival [7]. Nuclear stiffness is a determining factor for cancer progression and metastasis [8].

Nuclear rigidity and tight bonding to the cytoskeleton are required to sustain the functional and structural integrity of a cell [7, 9, 10]. Mutations in nuclear envelope proteins (e.g. lamin, nesprin), which determine nuclear stiffness and nuclear coupling to the cytoskeleton [11–13], lead to several diseases, including Emery–Dreifuss muscular dystrophy [14, 15], limb-girdle muscular dystrophy, and dilated cardiomyopathy [16]. Alterations in the nuclear matrix protein assembly can also cause several cancer types, including (human colon [17], bladder [18], benign prostatic hyperplasia, prostate [19], etc) Werner, Bloom, and Cockayne syndromes, and Fanconi anemia [20] diseases.

Generally, nature has designed DNA as a highly stable structure that protects cellular integrity, as seen by its high stability against external forces [21] and heating [22, 23]. The nucleus needs to be very robust against temperature changes because it comprises the genetic material. For instance, human cells might be exposed to low temperatures in a cold water bath or by eating ice, or to high temperatures in saunas or by drinking hot coffee. Indeed, the DNA double helix keeps its structural shape up to 70 °C [22] before losing its tertiary bounding and splitting into two strands. Only at temperatures above 80 °C is the double helix fully divided [22]. Thus, DNA polymers are much more thermo-resistant than most proteins in human cells, which often denature a few degrees above 40 °C [23]. To this end, small temperature changes tremendously affect the efficiency of many cellular functions or even stop them [24–26]. A constant body temperature in homeothermic animals, such as humans, is important since the temperature range for optimal cell function is very tight.

How the mechanical stability of the nucleus and cell body is connected to variations of temperature is hardly known. However, optical traps allow combined measurements of thermal and mechanical effects on living cells, as recently demonstrated by Kießling *et al* [27]. This study proposes the application of time-temperature-superposition to complex biological systems, such as whole cells. Besides a linear cellular response to fast temperature changes, cells have seen shown to behave unsteadily for long-term measurements in which cells adapt to

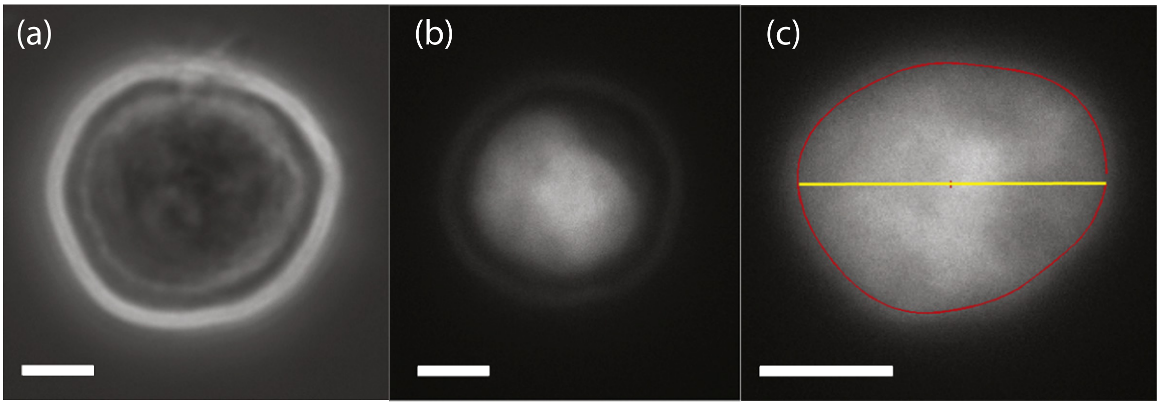

Figure 1. Single suspended MCF-7 cells optically trapped in the optical stretcher. (a) Phase contrast image. (b) Phase contrast image overlaid by a fluorescence microscopy image of the nucleus. (c) Close up of the fluorescently labeled nucleus. The red line indicates the detected nuclear edge. The yellow line represents the diameter in laser direction used for calculating the longitudinal deformation of the nucleus during the experiment. Scale bars represent 5 μm.

new thermal conditions. Nevertheless, temperature effects are usually neglected during measurements, and optical double beam traps have conventionally been used to probe mechanical properties of cells [28, 29]; for example, to study the influence of keratin to cellular stiffness [30] and to examine biomechanical differences between cancer and healthy cells [31, 32]. On the other hand, heating effects due to the absorption of the laser light by the cell in the optical trap can be used to trigger Ca^{+2} influx and to study its impact on cell stiffness [33]. As shown by Wetzel *et al* [34], the heating of cells in the optical trap does not cause apoptosis as long as the light exposure is short with laser powers below 2 W per laser fiber.

While the mechanical effects on the nucleus have been widely investigated [2, 7, 15, 35, 36], we report for the first time on the drastic impact of small temperature changes on the nucleus and the restructuring of its shape triggered by laser induced heating using a dual beam trap. *A priori*, due to the high thermoresistance of DNA, one might expect that the whole nuclear complex is similarly stable against heating. Here we show that the nucleus loses integrity at temperatures slightly above physiological temperatures. We find that temperatures above 45 °C already cause irreversible damage to the nucleus, which is accompanied by drastic and sudden changes in nuclear shape.

Although the nucleus in general is a strong and stiff structure, we find that cell nuclei exhibit a surprisingly low mechanical stability against heating. While damage occurs for different cell types at approximately the same transition temperature, the characteristics of the morphological changes of the nucleus induced by temperature turned out to be cell type specific. We investigate the thermal origin of nuclear restructuring, revealing differences when cells were heated quickly or slowly, and correlate nuclear instability to cell viability. Furthermore, the strong connectivity between cytoskeleton and nucleus becomes visible when the initial nuclear shape change propagates to the cytoplasm towards the cell membrane. Employing Latrunculin A as a drug to inhibit F-actin polymerization, our study demonstrates a new approach to investigate temperature induced intracellular force propagation between the nucleus, the cytoskeleton, and the external cell shape.

2. Materials and methods

2.1. Cell preparation

2.1.1. Cell culture. Mechanical changes, such as cell softening, have been established as a rheological signature distinguishing malignant cells from their normal counterparts [28, 30–32, 37, 38]. Moreover, recent work has shown the critical role that cell nuclei stiffness plays in metastasis [8]. Softer cell nuclei are a prerequisite for cancer cells to migrate through dense tissues [11]. It appears to be a common denominator that cancerous cells lose mechanical strength and show drastically altered nuclei [39].

Therefore, we have chosen commonly used normal and malignant breast cell lines to study the temperature stability of their nuclei. Most experiments were conducted with the malignant MCF-7 cell line (HTB-22). This epithelial breast cancer cell line was obtained from the American Type Culture Collection (ATCC, Manassas, VA). MCF-7 cells were maintained in 88% Eagle's Minimal Essential Medium, supplemented with 10 μg ml^{-1} insulin, 110 μg ml^{-1} sodium pyruvate, 10% fetal bovine serum, 1% penicillin/streptomycin, and 1% non-essential amino acids, all from Sigma-Aldrich (St. Louis, Missouri, US).

The other malignant cell lines that we used are MDA-MB-231 (HTB-26) and MDA-MB-436 (HTB-130), both obtained from ATCC. Both metastatic breast cell lines were cultured in the same medium composed of 90% Dulbecco's modified Eagle's medium (DMEM), 10% fetal calf serum (FCS), and 100 U/ml penicillin/streptomycin (all Sigma-Aldrich).

As normal reference MCF-10A (ATCC, CRL-10317), a non-tumorigenic epithelial cell line was used. Its culture medium contained a 1:1 mixture of Dulbecco's modified Eagle's medium and Ham's F12 medium, supplemented with 5% horse serum, 20 ng ml^{-1} epidermal growth factor, 10 μg ml^{-1} insulin, 100 ng ml^{-1} cholera toxin, 500 ng ml^{-1} hydrocortisone, and 100 U ml^{-1} penicillin/streptomycin (all Sigma-Aldrich). However, since MCF-10A is an immortalized cell line, it might also show characteristics found in malignant cells. Thus, HMEC cells (normal primary breast epithelial cells A10565), were obtained from Invitrogen (Life Technologies, Carlsbad, USA). The culture medium contained HuMEC Basal Serum Free Medium supplemented by 1% HuMEC supplement and 50 μg ml^{-1} bovine pituitary extract (Invitrogen).

2.1.2. Cell staining, drug treatment, and measurement. Prior to measurements, the cells were cultured in 25 cm^2 flasks. The cells were detached by application of 1 ml 0.0025% trypsin-EDTA solution, resuspended in 5 ml of culture medium, and centrifuged at 100 g for 4 min. In the end, single cells were resuspended in culture medium to a concentration of about 5*10^5 cells per ml and loaded into the optical stretcher.

Due to their poor visibility in phase contrast, the nuclei were stained using a standard dye and observed using fluorescence microscopy. The vital Hoechst 33 258 dye (Invitrogen/Molecular Probes, Cat. No. H21491) was used since it minimally interferes with the nucleus, providing good viability [40]. To label cell nuclei for observation, 10 μg ml^{-1} Hoechst was added to the cell medium one hour before detaching the cells from the culture dish to prepare a single cell suspension for the optical stretcher measurements. Furthermore, no Hoechst dye was added to the resuspended cell solution during the measurement.

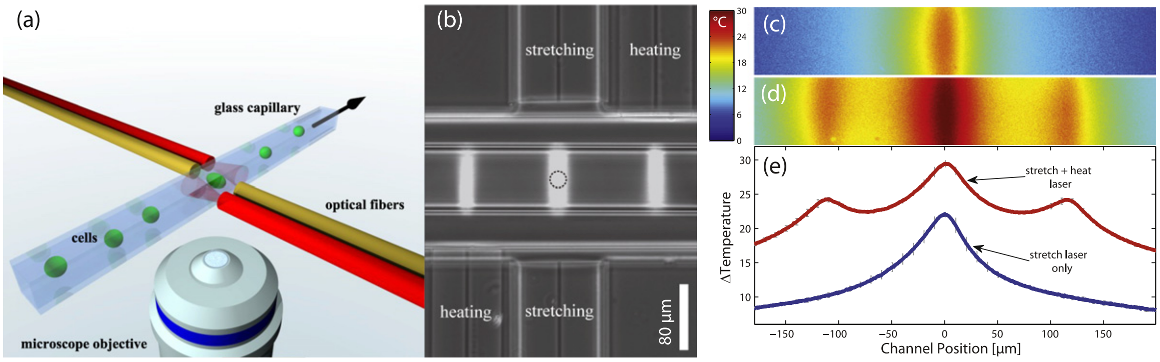

Figure 2. The optical stretcher and heat laser setup. (a) 3D sketch of the setup. Single suspended cells are transported through a square glass capillary placed perpendicularly to the optical fibers. Two counter-propagating 'stretch laser fibers' (yellow) form the classical optical stretcher trap, where the cells can be held and stretched by optical forces [43]. In our setup, the temperature of the trapped cells can be changed quickly by laser light emission of the additional 'heat laser fibers' (red). (b) The phase contrast image of the optical stretcher setup. The dashed circle indicates the size of a typical cell in the trap. The bright stripes in the capillary show emitted laser light. Although the heat laser light does not interact directly with trapped cells, it increases the temperature in the trapping region within milliseconds. Right: spatial temperature distribution measured in the capillary. In (c) only stretch lasers were activated at a power of 800 mW each. (d) Heat lasers additionally emitted a power of 1000 mW each. (e) The temperature distribution is plotted over the channel position. The blue curve reflects the situation in (c) and the red graph in (d), respectively. The temperature increasing factor of the stretch lasers was calculated to $\Delta T_s = 26\ \mathrm{K\,W^{-1}}$ (per fiber) and the temperature increasing factor of the heat lasers was $\Delta T_h = 7\ \mathrm{K\,W^{-1}}$ (per fiber). The figures are adapted from [27].

To investigate the influence of actin in the cytoskeleton, attached MCF-7 cells in culture were treated with 0.25 μM Latrunculin A (Sigma-Aldrich) for 8 hours to depolymerize the F-actin network. After trypsinization, Latrunculin A was kept in the cell suspension.

2.2. Optical stretcher with temperature controllable stage

We used an optical double beam trap, which is generally referred to as the automated optical stretcher. This is a valuable device to investigate the mechanical and thermal properties of single suspended cells with significant throughput (measurements of about 200 cells and nuclei per hour are possible). In this study, we mainly focused on the thermal properties of cell nuclei.

The optical stretcher setup generally consists of a small square glass capillary (80 μm inner diameter, 40 μm wall thickness, ST8508, VitroCom, USA), where the cells are pumped through. Two laser fibers (standard HI-1060 single mode fibers) are aligned perpendicularly, as shown in figure 2(a). The setup is mounted on an inverted Axio Observer Z1 microscope (Carl Zeiss, Jena, Germany), while the area in which cells are trapped ('trap-region') is magnified with a 63x air objective (Carl Zeiss, Jena, Germany). The cell images were recorded by a PHYTEC FireWire-CAM-111 H camera (PHYTEC, Mainz, Germany).

Single suspended cells were transported by microfluidic flow into the trap-region between two counter-propagating laser beams (laser wavelength: λ = 1064 nm (YLM-2-1064, IPG

Photonics, Germany)). Due to the higher refractive index of cells compared to the surrounding medium, the laser light refracts on the cell surface. The resulting forces, due to a small applied laser power (P_{trap} = 100 mW), trap cells stably between both laser beams (see figure 1(a)) [41].

Raising the laser power increases the effective temperature of cells due to light absorption. In the following experiments a linear increasing laser pattern was employed with a laser power increase of $\Delta P_{stretch} \approx 300$ mW s^{-1} corresponding to an increase of about 7.8 ± 1.2 K s^{-1}. Since an applied laser power of 1 W for each laser fiber leads to effective heating of about 26 ± 4 K [27, 42] (figure 2), the accompanied increase of stretching force (mainly acting on the outer cell surface) did not induce structural changes of the nuclei, as shown in section 3.3. After the laser power was switched off, the temperature of the medium in the trap-region returned to its initial value before the next cell was analyzed.

To analyze the nuclear shape and possible changes during laser induced heating we recorded fluorescence images of the cell nucleus during the time the cell was trapped and heated in the trap-region. The nuclear shape was later analyzed by a custom gradient-based edge detection algorithm written in MATLAB (Mathworks, US), similar to the algorithm described in [29].

A temperature controlled stage was used to adjust the various constant stage temperatures of the whole optical stretcher setup and the including cell container [27]. This enabled the investigation of cellular response to varying ambient temperatures in long-term temperature assays, within approximately 30 min. In addition, the stage temperature was kept stable at 23 °C for the other experiments.

2.3. Optical stretcher heat laser setup

Stretching cells in the optical stretcher has two effects: (1) a pulling force acts on the cell membrane, and (2) cells are heated due to laser light absorption within the cells and its surrounding medium. Another innovation for the examination of fast temperature effects is the use of two additional *heat laser* fibers (standard HI-1060 single mode fibers) aligned next to the *stretch laser* fibers (figure 2). Thus, by increasing the *heat laser* power, the effective temperature in the trap-region rises within milliseconds, without direct light exposure to the cells. Hence, we are able to analyze cellular and nuclear reactions to ultra-fast temperature jumps, where the cells do not have the time to adapt to the new ambient temperatures. The detailed setup, its temperature distribution, its temperature calibration, as well as extensive measurements on thermorheology of single cells were previously published by Kießling *et al* [27].

The temperature increase within the trap-region was determined for the stretch lasers $\Delta T_{stretch} = 26$ K W^{-1}, and for the heat lasers $\Delta T_{heat} = 7$ K W^{-1} per fiber, respectively (figure 2(e)).

3. Experimental results

3.1. Nuclear restructuring in the optical stretcher

To investigate the influence of heat on cell nuclei integrity, MCF-7 cells were trapped by two counter-propagating laser beams in the automated optical stretcher. While linearly increasing laser power, the fluorescently labeled nucleus was monitored. If the laser power increased as seen in figure 3(a), no visible deformation of nuclei occurred below a certain threshold laser power. Above

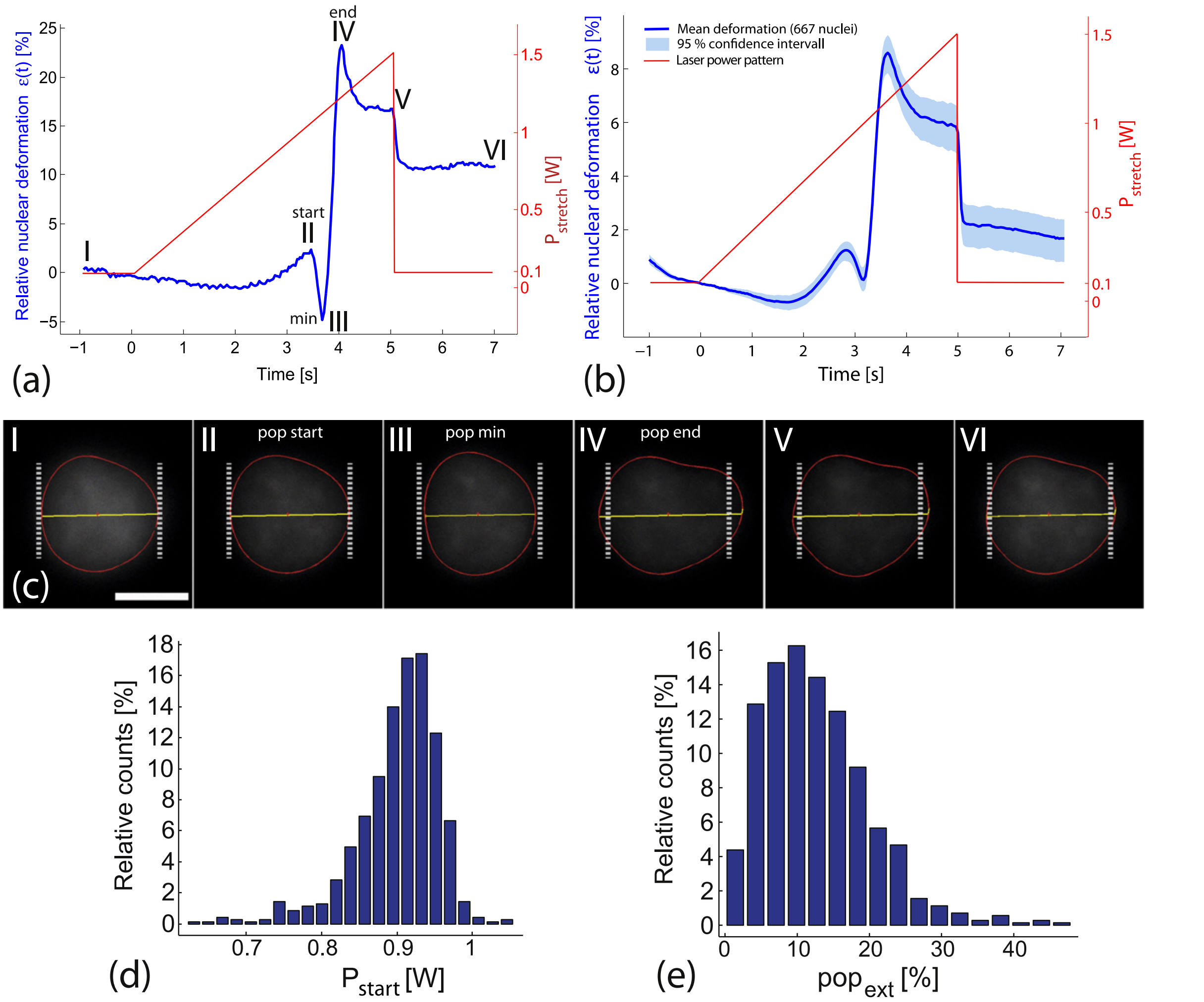

Figure 3. (a) Typical deformation curve of an individual MCF-7 cell nucleus (blue) in response to a linearly increasing stretch laser power (red). At low laser powers up to approximately t = 2.1 s ($P_{stretch} \approx 700$ mW corresponding $T_{eff} \approx 41$ °C), the nuclear width slightly decreases despite increasing optical stress. Subsequently, the nucleus starts to extend, indicating initial nuclear reshaping. During further temperature increase, the nuclear elongation reaches a local maximal value (II), further denoted as the starting point of the nuclear pop event ($T_{start} \approx 46.7$ °C) . Subsequently, the nucleus contracts to a minimal width (III) ($T_{min} \approx 49.1$ °C) followed by a drastic increase of nuclear elongation (≈ 30%) to a new local maximal value (IV) (corresponding to an effective temperature of $T_{end} \approx 52.0$ °C), where the nuclear pop ends. (b) Deformation data of 667 individual MCF-7 cell nuclei. The blue line shows the mean deformation and the surrounding patch indicates the 95% confidence interval. Note, this deformation curve is qualitatively similar to (a) while the extension of the mean elongation (from 'min' to 'end') is only about 9%. (c) Fluorescence images of the nucleus shown in (a) at characteristic points. The detected nuclear edge is shown in red, elongation in laser direction in yellow, and the initial diameter (t = 0) is indicated by dashed lines. The scale bar represents 10 μm. (d) Distribution of the pop start event (II) for 667 measured MCF-7 nuclei. (e) Shows the distribution for the pop extension (the nuclear elongation from minimal nuclear size (III) to maximal size (IV)).

this threshold the nuclei suddenly contracted and subsequently elongated significantly by approximately 10% towards the laser direction before reaching a new final shape. We term this sudden instability in longitudinal nuclear extension (axial elongation of the nucleus parallel to laser direction) *nuclear pop* due to its similarity to popcorn; compare figure 3 for a typical example.

A representative video of a nuclear pop is presented in the supporting material (see video S1, available at stacks.iop.org/njp/16/073009/mmedia). Structural reshaping of the nucleus was observed in 96 ± 3% of all examined MCF-7 cells. The remaining nuclei did not contract nor extended significantly but rather kept their shape without having a visible nuclear pop. For a quantification of the nuclear pop, we define certain characteristic points in the nuclear deformation curve, see figure 3. The initial nuclear contraction is denoted as the starting point of the nuclear pop, the corresponding laser power as pop start power (P_{start}). The associated effective temperature was calculated to $T_{start} \approx 47$ °C (as described in section 2.3). Alterations of the nuclear size between minimal and maximal nuclear elongation is termed *pop extension* and was determined to $pop_{ext} \approx 12\%$ for MCF-7 cells.

Interestingly, no correlations were observed between the nuclear volume and the characteristics of the nuclear pop (e.g. P_{start} or pop_{ext}) within the same populations of MCF-7 cells (data not shown).

To exclude an influence of the Hoechst dye to the nuclear pop, we examined MCF-7 cells without Hoechst dye application in phase contrast microscopy during laser exposure in the optical stretcher. The nuclear pop was still clearly observable, corroborating that the employed dye does not affect the nuclear pop.

3.2. Nuclear pop characteristics vary between different cell lines

We investigated several cell types under identical experimental conditions to evaluate if the nuclear pop occurs only for MCF-7 cells. Breast cancer cell lines, such as MCF-7, MDA-MB-231, and MDA-MB-436, as well as healthy breast cells, such as MCF-10A and primary human mammary epithelial cells (HMEC), were examined and compared.

Figure 4 displays observed nuclear deformation characteristics for all five cell types in response to the same heating conditions from identical linearly increasing laser power patterns in the optical stretcher.

HMEC cell nuclei showed a similar extension in nuclear deformation curves, as seen for the MCF-7 cells, while the average difference between minimum and maximum nucleus elongation is less pronounced with $pop_{ext} \approx 7\%$ (table 1). The nuclear pop started by an effective temperature of approximately 47 °C, as seen for MCF-7 cells. Again, about 94% of all nuclei showed nuclear instability. The nuclei of MDA-MB-436 and MDA-MB-231 cell lines exhibited a less pronounced nuclear contraction before the nuclear pop occurred. Only slight extensions in nuclear elongation during linear increasing laser power were observed. Detailed information are provided in table 1.

The smallest nuclear reshaping was observed for MCF-10A cells. As seen in figure 4, the nuclear deformations did not show characteristics of nuclear contraction and subsequent elongation.

It is remarkable that all of the reshaping nuclei expanded parallel to the laser axis before contracting and initiating the nuclear pop during optical heating. At a closer look, the details of nuclear pop characteristics are differently expressed in various cell types. We assume a different

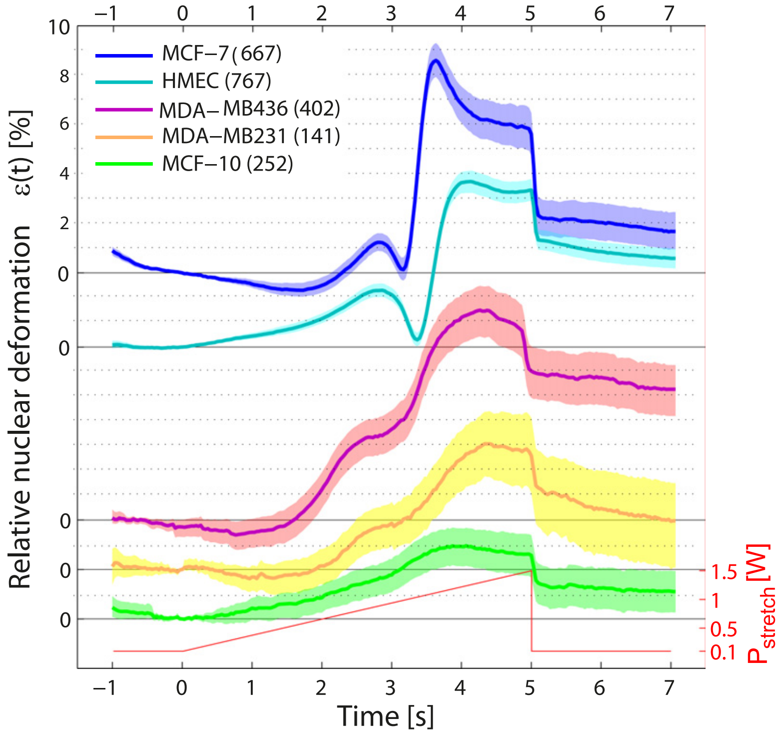

Figure 4. The mean deformation curves of four epithelial breast cell lines and primary HMEC cells. Despite being exposed to the same linearly increasing laser power (red), the characteristics of nuclear reshaping differ between cell types. MCF-7 (blue) and HMEC (cyan) showed most distinct nuclear reshaping with high extensions between minimal to maximal nuclear elongation. Both MDA-MB cell lines (436 in orange and 231 in pink) showed slight but significant nuclear contraction and subsequent elongation. For MCF-10A cells (green) no significant nuclear restructuring was observable. Nuclear instability starts between 2.5 and 3 s (corresponding to an effective temperature of T_{start} = 45 to 49 °C) reaching its equilibrium between 4 and 4.5 s (T_{end} = 57 to 61 °C). Patches around the mean curves indicate the 95% confidence interval.

assembly of the nuclear protein structure causing different nuclear pop characteristics, which might not be correlated to the cancer state of the cells. In the following, we investigated the nuclear pop event and how it is triggered in more detail.

3.3. Nuclear pop is triggered by heating

When laser light propagates from the cell culture medium into the cell, the momentum of the light increases, resulting in a pulling force acting on the cell surface due to conservation of momentum [41]. It might be expected that optically induced forces are responsible for the observed nuclear restructuring since the entire cell extends along the laser axis. However, the stretching forces are quite small, only about 10 Pa peak stress [43] is acting in the laser direction. In contrast, the cell nuclei are quite stiff with a Young's modulus of about 1 kPa [44]. The question arises, is the nuclear pop caused by laser light induced forces acting on the cell surface or by laser induced heating in the optical stretcher? Since the nuclear pop appears most conspicuous in MCF-7 cells, the following experiments refer to this cell type.

Table 1. Overview of investigated cell types ordered by the probability of nuclear reshaping (pop_{prob}). All measurements were conducted at T_{stage} = 23 °C. Most MCF-7 and HMEC cell nuclei show nuclear restructuring with the highest relative extension (pop_{ext}) in nuclear size (difference from minimal to maximal nuclear elongation). Both MDA-MB cell lines exhibit minor nuclear pop characteristics: only about half of all measured cells showed nuclear pops, with smaller pop extensions (pop_{ext}) too. Only about 5% of all MCF-10A cell nuclei are reshaped, showing only a small nuclear extension (pop_{ext}). T_{start}, T_{min}, and T_{end} yield an effective temperature of the initial contraction, minimal elongation, and the maximal elongation of the nuclear shape during the pop events. Values are medians with the mean deviation calculated by equation (1); compare with the mean graphs in figure 4.

Celltype	**pop**$_{prob}$	**T**$_{start}$ [°C]	**T**$_{min}$ [°C]	**T**$_{end}$ [°C]	**pop**$_{ext}$ [%]
MCF-7	95.7%	46.7 ± 1.0	49.1 ± 0.9	52.0 ± 1.0	11.5 ± 5.7
HMEC	94.4%	47.1 ± 1.2	50.5 ± 0.7	54.2 ± 1.2	7.1 ± 4.4
MDA-436	53.5%	46.7 ± 1.9	50.4 ± 1.5	55.6 ± 1.9	5.6 ± 3.8
MDA-231	38.6%	46.7 ± 2.3	49.6 ± 1.9	55.9 ± 2.3	3.9 ± 2.3
MCF-10A	4.8%	44.8 ± 1.6	47.0 ± 1.2	53.8 ± 2.2	3.1 ± 1.1

To test whether a mechanical pull on the cell body originates the sudden nuclear instability, bovine serum albumin (BSA) was added to the cell medium in the microfluidic channels. Thus, the refractive index of the cell medium was matched to the refractive index of the cellular cytosol, corresponding to n ≈ 1.36–1.39 [45–47]. Hence, mechanical pulling forces acting on the cell membrane and transmitting to the nucleus were minimized due to missing alterations of refractive indices.

Unexpectedly, the nuclear pop still occurred at slightly lower laser powers (≈ 96% of the laser power compared to measurements without BSA). Additionally, the used medium-BSA solution absorbs slightly (≈ 5%) more light than medium without BSA. Since the nuclear pop is triggered by lower laser power, in a medium with a higher absorption rate we assumed a similar threshold temperature inducing the nuclear pop, which is examined in the following.

3.3.1. Alteration of stage temperature. To verify that nuclear reshaping is a thermally triggered effect induced by a certain threshold temperature, we investigated the nuclear reaction by making alterations of the entire stage temperature in the optical stretcher. We heated the whole experimental stage in order to observe the nuclear pop for lower stretch laser powers. Briefly, the microscopy stage temperature, including the cells, was slowly increased from 18 °C to 38 °C in steps of 5 °C. MCF-7 cells had time to adapt to different stage temperatures for at least 30 min. For each stage, the temperatures of about 100 cells were measured by linearly increasing the laser power, leading also to higher effective temperatures (figure 5).

We observed that, for higher initial stage temperatures, lower laser powers are sufficient to induce the nuclear pop. We expected all nuclear pops to occur at the same effective temperature. However, a closer inspection of our data revealed that the effective temperature of nuclear reshaping (T_{start}) is not constant:

$$T_{start} = T_{stage} + \Delta T_{stretch} * P_{start} \neq const. \tag{1}$$

T_{stage} represents the constant temperature of the whole experimental optical stretcher stage. $\Delta T_{stretch}$ describes the temperature increase in the trap region due to light absorption, with a value

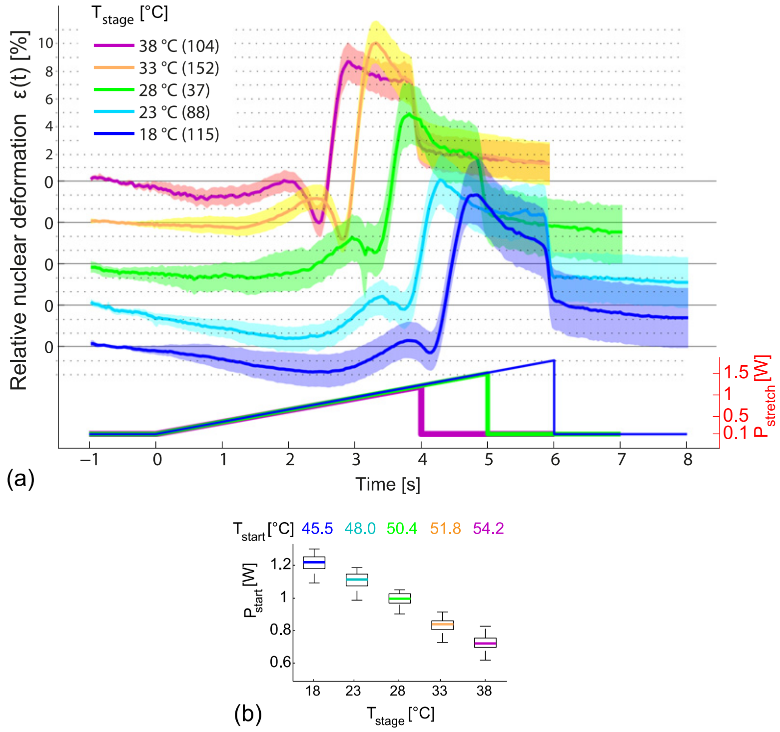

Figure 5. Nuclear instability of MCF-7 cells at different stage temperatures T_{stage} ranging from 18 °C to 38 °C. (a) Mean nuclear deformation curves as a response to linearly increasing laser power (bottom). Despite effective temperature increases in the same way, the nuclear pop event systematically shifts to lower stretch laser powers ($P_{stretch}$) for higher stage temperatures (T_{stage}). This clearly indicates a temperature dependence. (b) Boxplot of stretch laser powers for the pop start events at different stage temperatures. It is clearly visible that a higher initial stage temperature (T_{stage}) will require less laser power to start the nuclear pop event. The effective temperatures T_{start} for each T_{stage} were calculated. A higher initial temperature will require more additional heat, from laser power, to induce the nuclear pop; indicating that the cells and their nuclei are adapted to be more thermoresistant for higher environmental temperatures.

of 26 K W^{-1} (see Materials and methods). P_{start} is the corresponding laser power when the nucleus starts to contract. Multiplication of $\Delta T_{stretch}$ and P_{start} yields the temperature increase due to stretch laser absorption. For higher stage temperatures, the effective temperature of the nuclear pop increased from T_{start} (18 °C) = 45.5 ± 4 °C at 18 °C to T_{start} (38 °C) = 54.2 ± 4 °C at 38 °C stage temperature (figure 5). The increased nuclear pop temperature with increased exposition to higher stage temperatures suggests that cells can adapt to higher environmental temperature with time by employing a thermal protection mechanism; for instance, by inducing the expression of heat shock proteins for the better nuclear resistance of even higher temperatures. For further investigations it could be highly interesting to examine this adaptive process in more detail.

3.3.2. Fast heating by additional heat laser fibers. In contrast to the previously described experiment, we further studied to what extent fast heating influences nuclear restructuring when

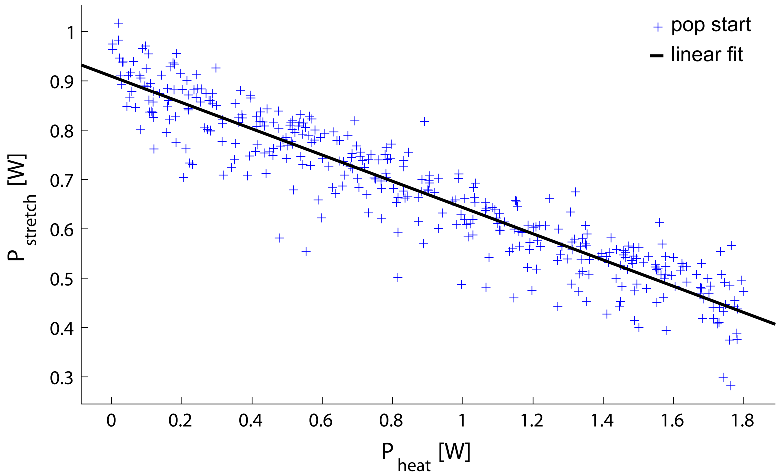

Figure 6. The nuclear pop event depends exclusively on temperature. 375 cells were measured with linearly increasing stretch laser power, with simultaneous ultra-fast heating of the trapping region by heat lasers. Heat lasers enabled fast alteration of initial temperatures, where cells could not adapt to the new ambient temperatures. The heat laser power was randomly chosen between 0 and 1.8 W for each cell individually. Blue crosses are stretch laser powers at which nuclei start to reshape. For higher heat laser powers (P_{heat}), lower stretch powers ($P_{stretch}$) were required to induce the nuclear pops. The black line is a linear fit yielding a slope of $m = -\frac{\Delta T_h}{\Delta T_s}$. All MCF-7 nuclei restructured at an effective temperature of $T_{start} = 46.7 \pm 0.4$ °C, if they were not able to adapt to initial thermal conditions.

the cells do not have the time to adapt to different stage temperatures. We employed a heat laser setup (see Materials and methods) utilizing additional lasers for fast temperature changes, as shown in figure 2. Heat lasers increase the temperature of the medium around the cells on a millisecond timescale, thus the cells do not have the time to adapt biologically to the new thermal conditions. The stage temperature was kept constant at 23 °C.

Simultaneously, the stretch laser increased steadily, as for all other experiments described previously. Heat lasers were activated at constant power during the whole data recording of every individual cell. For different cells, the heat laser powers were randomly selected, ranging from 0 up to 1800 mW. As more heat laser power was applied, the initial temperature of the cells in the trap rose.

As seen in figure 6, by using higher heat laser powers the starting event of the nuclear pop shifts linearly towards lower stretch laser powers. This trend supports our hypothesis: the warmer the initial cellular environment (caused by heat laser absorption), the lower the stretching power sufficient to induce nuclear shape changes. We calculate effective temperatures in the trap region required to start nuclear pops via:

$$T_{start} = T_{stage} + \Delta T_{stretch} {}^{*} P_{start} + \Delta T_{heat} {}^{*} P_{heat} \approx 46.7\ °\mathrm{C}.$$

This equation is based on equation (1) and extended by a factor describing heating due to heat laser absorption ($\Delta T_{heat} = 7$ °C/W is the temperature increasing rate in the trap-region due to heat laser light absorption as described in Materials and methods; P_{heat} is the applied heat laser power).

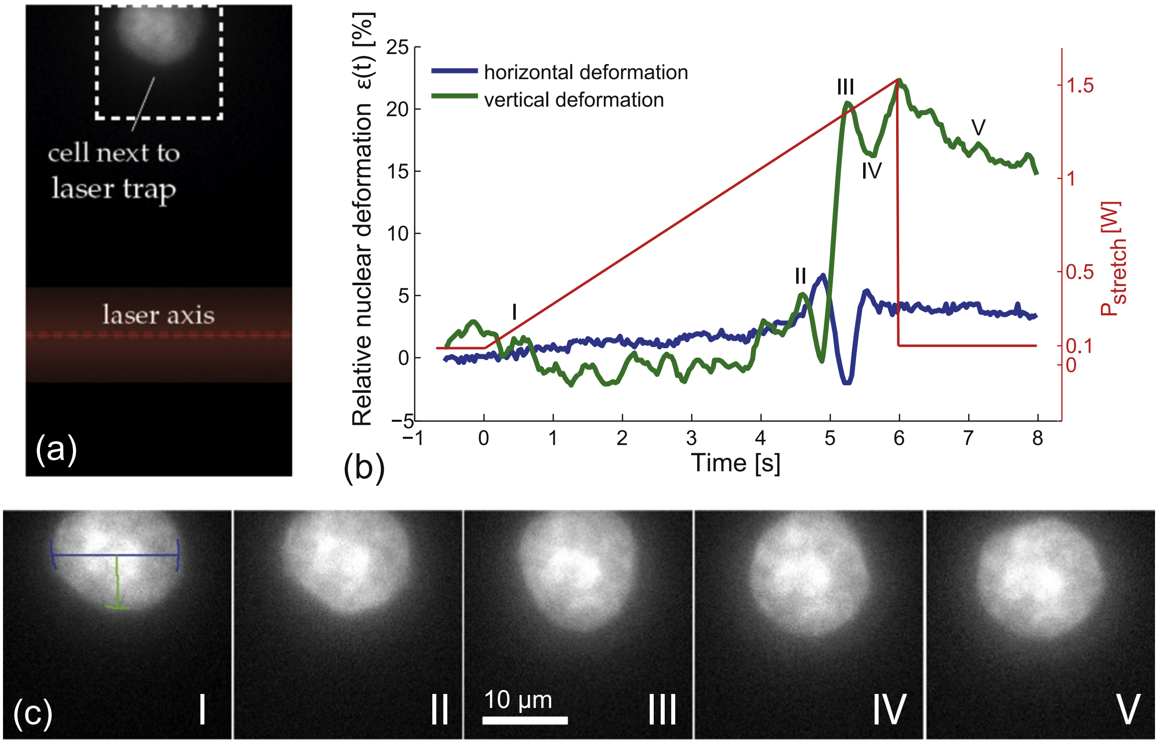

Figure 7. The direction of reshaping during the nuclear pop was not caused by optical forces but temperature gradients. (a) A cell (only the nucleus is visible) was positioned next to the laser axis where it was not exposed to laser light. (b) When the measurement region was heated until the nuclear pop occurs, the nucleus deformed mainly into the direction of higher temperatures. (c) Fluorescent images of the nuclear restructuring. The nuclear pop event starts at the point of highest temperature and subsequently propagates through the whole nucleus in a wavelike manner. As seen in (II) and (III), the nucleus elongates perpendicular to the laser axis. In this experiment no optical forces were exerted on the cell. A real time video of this cell is provided in the supporting material (see video S2, available at stacks.iop.org/njp/16/073009/mmedia).

Here, we see that if cells did not have time to adapt to a new stage temperature, the effective temperature at which nuclear instability occurred was constant. Hence, the nuclear pop is clearly a thermal effect.

3.3.3. Nuclear pop without direct light exposure. As ultimate proof that only temperature triggers the nuclear pop, we investigated nuclear reshaping without any direct laser exposure. Cells were transported next to the trap-region and they were subsequently allowed to settle down on the bottom of the glass capillary. Afterwards, the stretch laser power was switched on and linearly increased without direct laser light exposure to the cell. The cells only experienced a temperature increase in the surrounding medium and felt no optical forces at all.

As shown in figure 7, the nuclear contraction started on the stretch laser side and propagated through the whole nucleus like a thermal wave perpendicular to the laser axis. An example video is provided in the supporting material (see video S2, available at stacks.iop.org/njp/16/073009/mmedia). This experiment proves that only the temperature gradient is responsible for the nuclear pop and further explains its characteristic appearance (i.e. contraction and subsequent elongation).

3.4. Correlation of nuclear pop with cellular viability

The question arises if observed nuclear instability is reversible and how cell viability is affected.

3.4.1. Nuclear reshaping is irreversible. Optical inspection of the nuclear shape did not show any recovery after the pop. MCF-7 cells were exposed twice to the same linearly increasing stretch laser pattern. The nuclei reshaped during the first light exposure, while a second restructuring event of the same nuclei was not observed, even for a recovery time up to 20 min between both measurements. Hence, the nuclear pop seems to be an irreversible event and the cell nuclei do not recover their initial structure.

3.4.2. Thermally induced cell death. The irreversible nuclear instability raises the question if the cells are killed by laser induced heat shocks. Since cell sorting and subsequent cell re-cultivation of measured cells were not possible, cell viability as related to the nuclear pop was investigated indirectly. Cell adhesion after laser light exposure was employed as an indicator for cell viability. A detailed experimental procedure is explained in [34]. Briefly, the microscopy stage was heated to 37 °C to provide physiological conditions. MCF-7 cells were stretched by a linearly increasing laser ramp. Subsequently, the cells were allowed to settle down on the bottom of the glass capillary. Since there was no microfluidic flow in the capillary, viable cells would have started to adhere to the substrate within minutes. We found that after nuclear reshaping the cells rarely adhered to the capillary. In contrast, the control cells quickly attached and spread to the capillary ground.

In a further approach to examine possible correlations between cell viability and nuclear pop, the cells were preheated in a water bath prior to investigation in the optical stretcher. The cell suspension (about $5*10^5$ single cells in 1 ml medium) was kept in a temperated water bath for 5 min at different temperatures ranging from 46 to 54 °C. Subsequently, the cells were split into two subpopulations. The first population was recultured in a new culture dish to obtain the survival rate of cells after heat treatment. The second population was measured in the optical stretcher by applying the standard linearly increasing laser pattern. The nuclear deformation curves as well as survival rates for the various preheated cells are plotted in figure 8.

After exposure to temperatures up to 48 °C, most cells survived in cell culture. Significant differences in nuclear deformation curves of the population measured in the optical stretcher were not observed. In contrast, heat treatment of 50 °C in the water bath initiated cell death for the majority of cells. Only about 10% of cells adhered to the substrate in post cell cultivation, indicating hyperthermic cell death [48]. The remaining cells maintained a round shape even after several days of culture. However, for these cells the characteristic nuclear pops were clearly observable, as similarly seen for cells pretreated at 52 °C. Although all of the cells were dead in the cell culture at 52 °C, they still exhibited clear laser induced nuclear reshaping. Only if the cells experienced a temperature of 54 °C for 5 min did the nuclear pop behavior, in particular nuclear contraction and subsequent elongation, vanish in the nuclear deformation curves (figure 8). Thereby, the all-over shape of the suspended cells after the heat bath in the optical stretcher was not different to that of the healthy control cells.

Another correlation of dead cells and nuclear pop characteristics arose in all optical stretcher experiments. Any cell suspension contained a small fraction of unavoidably dead cells due to trypsinization and centrifugation prior to measurements, for instance. Dead cells were clearly recognizable in the phase contrast images by an overall low contrast and fuzzy contours,

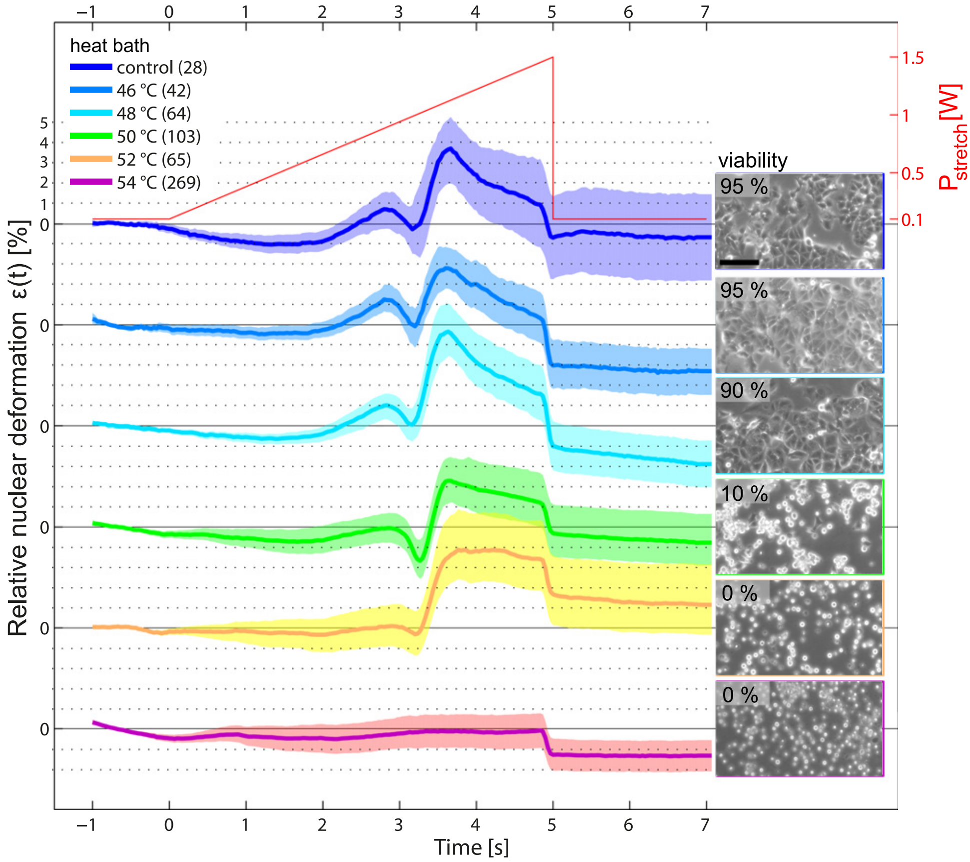

Figure 8. Nuclear deformation of MCF-7 cells after 5 min exposure to different heat bath temperatures. Control represents the mean deformation curve of stretched nuclei without heat exposure prior to measurement. Up to 48 °C (bright blue curves), preheated cells reveal nuclear characteristics similar to the control. The nuclei of cells heated to 50 °C (green) in advance to the measurement significantly lost viability in post-cultivation, while the nuclear pop extension still showed similar characteristics to the control. Cells heated to 52 °C (orange) did not adhere at all in further cultivation, whereas nuclear pop characteristics slightly differed from control cells. In contrast, the cells lost all nuclear pop characteristics after being heated to 54 °C (pink) indicating denaturation of certain structure proteins in the nuclei, which are probably related to nuclear reshaping. Right: phase contrast images of cells in post-cultivation, seeded after the heat bath exposure. The higher the temperature of the heat bath, the fewer cells adhered to the substrate, indicating less cells surviving. After 50 °C (green), dead cells mostly showed a bright round fixed shape. The scale bar represents 100 μm.

as well as in the fluorescence microscopy images where nuclei were abnormally bright. During all of the measurements of untreated and preheated cells, we never observed that nuclei of dead cells reshaped upon heat exposure by the lasers beams, rather they kept their round shape. These observations strongly suggest that the nuclear pop induces cell death. However, some hyperthermic damaged cells still accommodate intact nuclei, showing laser induced nuclear reshaping.

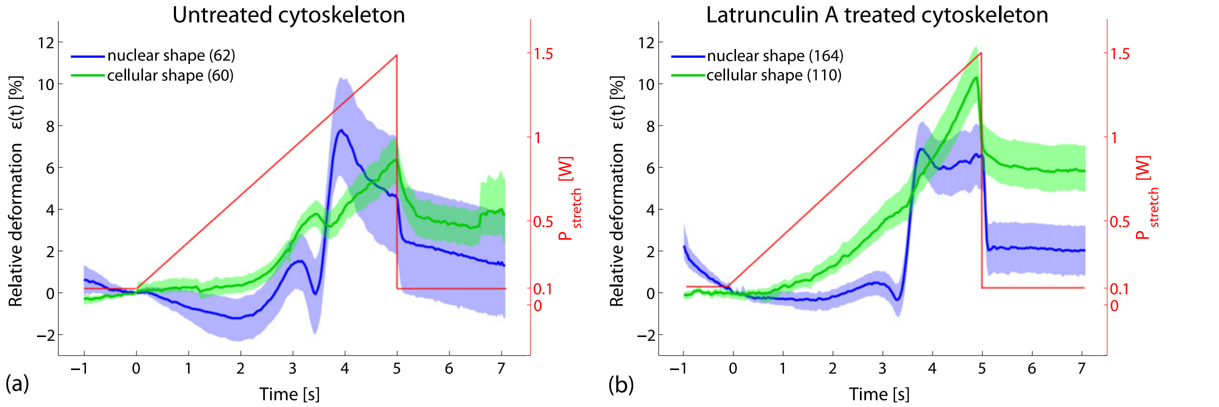

Figure 9. Deformation curves of MCF-7 cells (green) and of their nuclei (blue), untreated (a), and treated with Latrunculin A (b). The corresponding stretch laser power in the optical stretcher is indicated by the red line. (a) The whole-cellular response (green) was clearly affected by the nuclear pop event. (b) Inducing the rupture of cellular actin by Latrunculin A suppressed nuclear stress propagation through the cytoskeleton to the outer cell shape. The whole cell deformation (green) appeared less affected by the nuclear pop event. Yet the nuclear deformation of cells with disturbed actin network (b) was comparable to the nuclear deformation of untreated cells (a).

3.5. Mechanical force propagation between the nucleus, cytoskeleton, and outer cell body

The nucleus is not a mechanically independent body. It is associated with the cytoskeleton, the cell membrane, and even the extracellular matrix [49]. Cell nuclei are exposed to mechanical forces from outside cells, which are transmitted through the cytoskeletal meshwork. Moreover, forces are also generated inside the cell, such as during migration or cell division [50, 51], as well as due to recently observed nuclear rotations within an intact actin network [52]. Fast force propagation within the cell is enabled by the prestressed cytoskeletal network [53]. The molecular mechanisms by which cells mechano-sense and act to changes in their physical micro-environment needs further clarification. A detailed overview on how the nucleus is connected to these processes can be found in [9, 54].

We were able to correlate the reshaping of the nucleus by fluorescence images and deformations of the outer cell shape from phase contrast imaging. MCF-7 cells were exposed to steadily increasing laser powers, comparing the mean values of nuclear deformation (recorded by fluorescence microscopy) with the mean of cellular deformation (recorded by phase contrast microscopy). As seen in figure 9(a), a strong and time delayed reaction of the cell membrane was observed, presumably caused by tight connections of nucleus, cytoskeleton, and cell membrane. The outer cell shape followed nuclear contraction. Meanwhile, after the pop event the outer cell shape further expanded.

By employing cross-linkers, actin filaments form a highly organized, isotropic, bundled and branched network [55], establishing a link between nuclei and cell membranes [54]. To study the role of the actin cytoskeleton during nuclear and subsequent cellular reshaping, we added Latrunculin A (Lat A) to the cells 8 hours prior to measurements. Lat A sequesters actin monomers, preventing polymerization of actin filaments. This disturbance leads to disruption of the actin cytoskeleton and a loss of all-over integrity of the entire cytoskeleton [56]. Comparing untreated MCF-7 control cells with Lat A treated cells, the strong influence of actin in cytoskeletal force propagation is clearly visible (figure 9). Cell shape firmly follows nuclear restructuring for the case of an intact cytoskeleton. In contrast, in a dissolved actin cytoskeletal structure, the cell diameter expanded steadily in the direction of the laser axis without following the internal contraction and subsequent elongation of the nucleus. Only a response to optical stretching forces was observed in terms of an elongation of the entire cell along the laser axis. We note that the drug treatment did not affect the nuclear pop (blue curves in figure 9) since nuclear reshaping is qualitatively identical for Lat A treated and untreated MCF-7 cells. As shown previously, nuclear deformation and reshaping are not induced or impaired by the optical stretching. Only laser light induced heating can cause this effect. Thus, internal forces originating from the nucleus affect the shape of the outer cell membrane by force propagation through the actin cytoskeleton.

4. Discussion

In this study, the nuclear response of single suspended cells to local optical stretching and heating was investigated. Here, we observed a drastic and up to now unreported reshaping of cell nuclei caused by temperature rise. Even though it is not surprising that a certain temperature kills cells and destroys their protein assembly, the dynamics of the nuclear reshaping during heat exposure is a surprising phenomenon since the nuclear pop occurs already at temperatures barely above physiological conditions. We demonstrated that nuclear restructuring is triggered by: (1) a slow temperature increase induced by changing the stage temperature while stretching, (2) a fast heating of the trap region by additional heat lasers while stretching, and (3) even without direct light exposure when cells were exposed only to a heat bath. In particular, the correlation between heat waves propagating through the nucleus leading to nuclear reshaping verifies the causality of thermal and structural change.

Our results are corroborated by a recent study by Chalut *et al*, who investigated nuclear responses in the optical stretcher for embryonic stem cells of mice [57]. However, there is a significant discrepancy concerning the explanation of the origin of nuclear deformations of stem cells compared to fully differentiated cells. Chalut *et al* attribute the different nuclear deformations to differences in nuclear mechanical deformability. Thus, they did not consider the inherently present effect of thermal heating. However, in agreement with our conclusions, the authors stated that 'nuclear mechanics should be considered a significant agent of whole-cell mechanics'. In our study, we demonstrated for the first time that nuclear responses are independent of the cytoskeletal structure in terms of F-actin network integrity. This was similarly proposed by Chalut *et al*, who stated that 'nuclear deformation is insensitive to the mechanical properties of the cytoplasm'.

We found that thermal heating, even by a few degrees, generally had a significant effect on cell nuclei. We observed that heat exposure of fully differentiated cell nuclei drastically affects the nuclear shape and that responses vary substantially between different cell types. The observed nuclear instability due to heating might be attributed to heat-induced protein unfolding [24, 58] as well as nuclear protein aggregation [59] and reorganization of chromatin domains [60].

The nucleus consists mostly of DNA double strands, which are mechanically stable and start melting at 70 °C [22–24]. Since we observed the nuclear pop at much lower temperatures, more appropriate candidates involved in the reshaping event might be proteins responsible for nuclear organization and structural maintenance, such as histone proteins. These proteins structure and compact DNA double strands and facilitate packing in the dense nucleus [61]. However, Lepock *et al* observed that histones begin to unfold and lose their functionality above 60 °C [24]. However, this regime is too high to explain observed alterations concerning the nuclear shape starting between 42 and 48 °C.

Lamin proteins are located under the nuclear envelope, and sustain nuclear shape and stability [62]. Falloon *et al* reported in 2002 that temperatures between 42 and 45.5 °C cause distortions in the perinuclear lamina, as for instance invaginations in the envelope which might correlate to our heat induced nuclear contractions. Thus, the nuclear lamin proteins might be potential candidates to be involved in the nuclear pop mechanism. Further studies would be required to address this issue. However, we do not expect structural reorganization of only lamin proteins in the nuclear envelope to result in such drastic nuclear extension up to 30% of initial nuclear size, as observed in our experiments.

Restructuring and distortion of other nuclear proteins might be involved in the observed effects. Nuclear matrix proteins (NMPs) are spread and branched throughout the whole nucleus, providing stability by their dynamic network and help in organization such as gene expression [4, 63]. It is more likely that such proteins, which form structural networks branched throughout the entire nucleus, cause such drastic instability of the whole nuclear shape. Indeed, Lepock *et al* stated that the nuclear matrix seems to be the most thermolabile protein complex in the nucleus and that irreversible denaturation starts between 42 and 50 °C [64]. This regime is in good agreement with our observations.

Variations in the content of NMPs in different cell types might also be responsible for the different reshaping characteristics found in various breast cancer and normal breast cell types, such as MCF-7, MCF-10A, MDA-MB-231, MDA-MB-436, and HMEC cells. Although cancer cell nuclei are known to differ to healthy cell nuclei regarding their shape, size, margin, chromatin organization, nucleoli, nuclear matrix and nuclear membrane assembly [39], a correlation of the nuclear pop with malignancy is not observable for our measured cell types. For instance, distinct nuclear instability is observable for malignant (MCF-7), as well as for benign cells types (HMEC); see figure 4. While thermal failure of NMPs might explain the sudden elongation of the nucleus, the initial contraction prior to reshaping of the nucleus cannot be explained in that picture. The nuclear matrix can be described as a prestressed network in which thermal failure of important structure proteins causes a release of stored mechanical energy leading to a contraction of the nucleus. However, such a mechanism is speculative at this point and needs to be addressed in detail in the future. Further experiments should investigate the molecular processes and the involved proteins to gain a better understanding of the nuclear pop from a biological point of view.

The observation that only heat induces the nuclear reshaping is sustained by experiments in which single cells were exposed to heat via heat lasers or a heat bath prior to measurements. All of the cells exhibited a clear heat dependence. For higher initial stage temperatures the effective pop temperature that induced the nuclear pop also increased slightly (see figure 5). These findings indicate that cells react and adapt to higher environmental temperatures potentially by heat shock proteins (HSPs) [24]. Although HSPs protect cellular and nuclear function against heat damage, high temperatures lead to protein denaturation and aggregation. These proteins lose their functions, eventually leading to dysfunctions within the nucleus and in the end to cell death [59].

Temperature induced cell death of MCF-7 cells already begins at 43 °C when cells are exposed to heat for at least 2 hours, as reported by Ciocca *et al* [26]. In our experiments, MCF-7 cells were still viable after exposure to temperatures of up to 48 °C for 5 min. They adhered and spread during culture after heat exposure and no alterations in nuclear reshaping was observed. This behavior can be understood by considering protein denaturation as a rate dependent process. Cells exposed to low temperatures yet still above the denaturation temperature exhibit a reduced denaturation rate compared to cells at higher temperatures [65]. Thus, cells exposed to a heat bath for a few minutes can survive even higher temperatures due to the shorter exposure time compared to cells exposed to heat for hours.

We investigated the cellular viability and correlated thermal properties of nuclei in a heat bath, ranging from 48 to 54 °C for 5 min. Our results revealed two different heat responses. Firstly, the cells started to undergo cell death after exposure to a 50 °C water bath. Subsequently, they were no longer able to adhere to the culture dish. Nevertheless, the nuclei still exhibited a clear apparently intact structure, as observed with fluorescence microscopy, and showed characteristics of the nuclear pop in the optical stretcher. Secondly, more severely damaged cells resulted from higher heat bath temperatures of about 54 °C. This temperature regime caused denaturation and the nuclear pop was no longer visible. Interestingly, the cells appeared to be 'fixed' by the heat bath. Even after 2 weeks in culture, the cells were spherical and had a strong contrast in phase contrast microscopy, while they did not adhere to the culture dish. We propose that after 5 min at 54 °C all cellular processes are completely stopped, which normally dissolves cells leading to a blurred appearance. We expect that hyperthermic damage appears to take over cellular processes at temperature treatment up to 50 °C for 5 min, while the nuclear structure is still maintained. At temperatures of 54 °C both the nuclei and nuclear networks immediately lose their function.

For MCF-7 cells, we compared the interconnection of an intact cytoskeleton with a dissolved F-actin meshwork. The nuclear size and shape were similar in both populations, indicating that the ruptured actin skeleton does not release enough energy to significantly affect the stiff nucleus. The nuclear pop is an internal nuclear effect, releasing higher forces against the cytoskeleton than the cytoskeleton against the nucleus. The Latrunculin A (Lat A) treated cells were softer and lost structural stability, which is evident since the nuclear pop barely affects the outer cell shape 9. A closer look revealed a time lag of the force propagation from the nucleus to the outer cell membrane. We observed that the force wave of the nuclear pop reaches the membrane slightly faster in an unimpaired cell than in a cell treated by Lat A. As obtained from our experiment, a less branched scaffold provides less tensegrity, resulting in slower and weaker force propagation.

A detailed molecular investigation is still lacking to the extent of which and how nuclear proteins are involved in a heat induced nuclear pop. An explicit molecular correlation of involved proteins is difficult and might be worth trying to compare nuclear protein content before and after restructuring by simultaneous Raman spectroscopy [66]. Since we showed that the nuclear deformation curves are characteristic for different cell types, they might thus be employed as a cellular marker. Further knowledge of cytoskeletal architecture and interconnection can be gained from studies of the force propagation between nuclei and surrounding cell membranes.

Our results show that cell nuclei become unstable at amazingly small thermal disturbance, raising the question of how an organism deals with a thermal instability of the nucleus. Considering the relatively small energies that disintegrate the nucleus, it might be expected that nuclear structure can be also damaged when a metastatic cell squeezes through narrow spaces.

This does not seem to be the case. Thus, a temperature increase seems to have a unique effect on cells and needs further investigation, especially for a better understanding of the underlying processes during hyperthermia therapy, such as for cancer treatment.

Acknowledgments

We thank Kris Noel Dahl for helpful discussions, Steve Pawlizak for 3D rendering, and Tina Händler for the initial experiments. Financial support was provided in part by the German Science Foundation (DFG) KA 1116/9-1 and FOR 877, the European Union, and the Free State of Saxony. The Leipzig Graduate School of Natural Sciences 'Building with Molecules and Nano Objects' (BuildMoNa), established within the German Excellence Initiative, is further acknowledged.

References

[1] Fraser P and Bickmore W 2007 Nuclear organization of the genome and the potential for gene regulation *Nature* **447** 413–7

[2] Lombardi M L, Zwerger M and Lammerding J 2011 Biophysical assays to probe the mechanical properties of the interphase cell nucleus: substrate strain application and microneedle manipulation *J. Visualized Exp.* **55** PMID: 21946671

[3] Caille N, Thoumine O, Tardy Y and Meister J-J 2002 Contribution of the nucleus to the mechanical properties of endothelial cells *J. Biomech.* **35** 177–87

[4] Tsutsui K M, Sano K and Tsutsui K 2005 Dynamic view of the nuclear matrix *Acta Med. Okayama* **59** 113–20 PMID: 16155636

[5] Luger K 2003 Structure and dynamic behavior of nucleosomes *Curr. Opin. Genet. Dev.* **13** 127–35

[6] Chakravarthy S, Park Y-J, Chodaparambil J, Edayathumangalam R S and Luger K 2005 Structure and dynamic properties of nucleosome core particles *FEBS Lett.* **579** 895–8

[7] Martins R P, Finan J D, Guilak F and Lee D A 2012 Mechanical regulation of nuclear structure and function *Ann. Rev. Biomed. Eng.* **14** 431–55 PMID: 22655599 PMCID: PMC3575008

[8] Friedl P, Wolf K and Lammerding J 2011 Nuclear mechanics during cell migration *Curr. Opin. Cell Biol.* **23** 55–64

[9] Dahl K N, Ribeiro A J S and Lammerding J 2008 Nuclear shape, mechanics, and mechanotransduction *Circ. Res.* **102** 1307

[10] Houben F, Ramaekers F C S, Snoeckx L H E H and Broers J L V 2007 Role of nuclear lamina-cytoskeleton interactions in the maintenance of cellular strength *Biochim. Biophys. Acta* **1773** 675–86 PMID: 17050008

[11] Lombardi M L and Lammerding J 2010 Altered mechanical properties of the nucleus in disease *Meth. Cell Biol.* **98** 121–41 PMID: 20816233

[12] Zhong Z, Wilson K L and Dahl K N 2010 Beyond lamins: other structural components of the nucleoskeleton *Meth. Cell Biol.* **98** 97–119

[13] Crisp M, Liu Q, Roux K, Rattner J B, Shanahan C, Burke B, Stahl P D and Hodzic D 2006 Coupling of the nucleus and cytoplasm: role of the LINC complex *J. Cell Biol.* **172** 41–53 PMID: 16380439

[14] Schirmer E C and Foisner R 2007 Proteins that associate with lamins: many faces, many functions *Exp. Cell Res.* **313** 2167–79 PMID: 17451680

[15] Lammerding J, Fong L G, Ji J Y, Reue K, Stewart C L, Young S G and Lee R T 2006 Lamins A and C but not lamin B1 regulate nuclear mechanics *J. Biol. Chem.* **281** 25768–80 PMID: 16825190

[16] Worman H J, Fong L G, Muchir A and Young S G 2009 Laminopathies and the long strange trip from basic cell biology to therapy *J. Clin. Invest.* **119** 1825–36 PMID: 19587457 PMCID: PMC2701866

[17] Keesee S K, Meneghini M D, Szaro R P and Wu Y J 1994 Nuclear matrix proteins in human colon cancer *Proc. Natl. Acad. Sci. USA* **91** 1913–6 PMID: 8127905

[18] Getzenberg R H, Konety B R, Oeler T A, Quigley M M, Hakam A, Becich M J and Bahnson R R 1996 Bladder cancer-associated nuclear matrix proteins *Cancer Res.* **56** 1690–4

[19] Partin A W, Pound C R, Clemens J Q, Epstein J I and Walsh P C 1993 Serum PSA after anatomic radical prostatectomy. The Johns Hopkins experience after 10 years *Urol. Clin. N. Am.* **20** 713–25 PMID: 7505980

[20] Sjakste N and Sjakste T 2005 Nuclear matrix proteins and hereditary diseases *Russ. J. Genet.* **41** 221–6

[21] Clausen-Schaumann H, Rief M, Tolksdorf C and Gaub H E 2000 Mechanical stability of single DNA molecules *Biophys. J.* **78** 1997–2007 PMID: 10733978 PMCID: PMC1300792

[22] Movileanu L, Benevides J M, Thomas G J Jr and George J 2002 Temperature dependence of the Raman spectrum of DNA. II. Raman signatures of premelting and melting transitions of poly(dA).poly(dT) and comparison with poly(dA-dT).poly(dA-dT) *Biopolymers* **63** 181–94 PMID: 11787006

[23] Liu F, Tøstesen E, Sundet J K, Jenssen T-K, Bock C, Jerstad G I, Thilly W G and Hovig E 2007 The human genomic melting map *PLoS Comput. Biol.* **3** e93

[24] Lepock J R 2005 How do cells respond to their thermal environment? *Int. J. Hyperthermia* **21** 681–7 PMID: 16338849

[25] Parsell D A and Lindquist S 1993 The function of heat-shock proteins in stress tolerance: degradation and reactivation of damaged proteins *Ann. Rev. Genet.* **27** 437–96 PMID: 8122909

[26] Ciocca D R, Fuqua S A, Lock-Lim S, Toft D O, Welch W J and McGuire W L 1992 Response of human breast cancer cells to heat shock and chemotherapeutic drugs *Cancer Res.* **52** 3648–54 PMID: 1617638

[27] Kiessling T R, Stange R, Käs J A and Fritsch A W 2013 Thermorheology of living cells–impact of temperature variations on cell mechanics *New J. Phys.* **15** 045026

[28] Guck J *et al* 2005 Optical deformability as an inherent cell marker for testing malignant transformation and metastatic competence *Biophys. J.* **88** 3689–98

[29] Lincoln B, Wottawah F, Schinkinger S, Ebert S and Guck J 2007 High-throughput rheological measurements with an optical stretcher *Meth. Cell Biol.* **83** 397–423

[30] Seltmann K, Fritsch A W, Käs J A and Magin T M 2013 Keratins significantly contribute to cell stiffness and impact invasive behavior *Proc. Nat. Acad. Sci.* **110** 18507

[31] Runge J, Reichert T, Fritsch A, Käs J, Bertolini J and Remmerbach T 2013 Evaluation of single-cell biomechanics as potential marker for oral squamous cell carcinomas: a pilot study *Oral Dis.* **20** e120–7

[32] Fritsch A, Hockel M, Kiessling T, Nnetu K D, Wetzel F, Zink M and Käs J A 2010 Are biomechanical changes necessary for tumour progression? *Nat. Phys.* **6** 730–2

[33] Gyger M, Rose D, Stange R, Kießling T, Zink M, Fabry B and Käs J A 2011 Calcium imaging in the optical stretcher *Opt. Exp.* **19** 19212–22

[34] Wetzel F, Rönicke S, Müller K, Gyger M, Rose D, Zink M and Käs J 2011 Single cell viability and impact of heating by laser absorption *Eur. Biophys. J.* **40** 1109–14

[35] Maniotis A J, Chen C S and Ingber D E 1997 Demonstration of mechanical connections between integrins, cytoskeletal filaments, and nucleoplasm that stabilize nuclear structure *Proc. Nat. Acad. Sci.* **94** 849–54

[36] Rowat A C, Jaalouk D E, Zwerger M, Ung W L, Eydelnant I A, Olins D, Olins A, Herrmann H, Weitz D A and Lammerding J 2013 Nuclear envelope composition determines the ability of neutrophil-type cells to passage through micron-scale constrictions *J. Biol. Chem.* **288** 8610–8 PMID: 23355469

[37] Kumar S and Weaver V M 2009 Mechanics, malignancy, and metastasis: The force journey of a tumor cell *Cancer Metastasis Rev.* **28** 113–27

[38] Brunner C, Niendorf A and Käs J A 2009 Passive and active single-cell biomechanics: a new perspective in cancer diagnosis *Soft Matter* **5** 2171–8

[39] Dey P 2010 Cancer nucleus: morphology and beyond *Diag. Cytopathol.* **38** 382–90 PMID: 19894267

[40] Darzynkiewicz Z, Robinson J P and Crissman H A 1994 *Flow Cytometry* (Academic Press)

[41] Guck J, Ananthakrishnan R, Cunningham C C and Käs J 2002 Stretching biological cells with light *J. Phys.: Condens. Matter* **14** 4843
[42] Ebert S, Travis K, Lincoln B and Guck J 2007 Fluorescence ratio thermometry in a microfluidic dual-beam laser trap *Opt. Express* **15** 15493–9
[43] Guck J, Ananthakrishnan R, Mahmood H, Moon T J, Cunningham C C and Käs J A 2001 The optical stretcher: A novel laser tool to micromanipulate cells *Biophys. J.* **81** 767–84
[44] Guilak F, Tedrow J R and Burgkart R 2000 Viscoelastic properties of the cell nucleus *Biochem. Biophys. Res. Commun.* **269** 781–6 PMID: 10720492
[45] Choi W, Fang-Yen C, Badizadegan K, Oh S, Lue N, Dasari R R and Feld M S 2007 Tomographic phase microscopy *Nat. Meth.* **4** 717–9
[46] Curl C L, Bellair C J, Harris T, Allman B E, Harris P J, Stewart A G, Roberts A, Nugent K A and Delbridge L M D 2005 Refractive index measurement in viable cells using quantitative phase-amplitude microscopy and confocal microscopy *Cytometry Part A* **65A** 88–92
[47] Beuthan J, Minet O, Helfmann J, Herrig M and Müller G 1996 The spatial variation of the refractive index in biological cells *Phys. Med. Biol.* **41** 369
[48] Lepock J R 2003 Cellular effects of hypothermia: relevance to the minimum dose for thermal damage *Int. J. Hyperthermia* **19** 252–66
[49] Huber F, Schnauß J, Rönicke S, Rauch P, Müller K, Fütterer C and Käs J 2013 Emergent complexity of the cytoskeleton: from single filaments to tissue *Adv. Phys.* **62** 1–112
[50] Mierke C T, Rösel D, Fabry B and Brábek J 2008 Contractile forces in tumor cell migration *Eur. J. Cell Biol.* **87** 669–76 PMID: 18295931
[51] Walczak C E and Heald R 2008 Mechanisms of mitotic spindle assembly and function *Int. Rev. Cytol.* **265** 111–58 PMID: 18275887
[52] Kumar A, Maitra A, Sumit M, Ramaswamy S and Shivashankar G V 2014 Actomyosin contractility rotates the cell nucleus *Sci. Rep.* **4** 3781 PMID: 24445418 PMCID: PMC3896915
[53] Ingber D E 2003 Tensegrity I. Cell structure and hierarchical systems biology *J. Cell Sci.* **116** 1157
[54] Wang N, Tytell J D and Ingber D E 2009 Mechanotransduction at a distance: mechanically coupling the extracellular matrix with the nucleus *Nat. Rev. Mol. Cell Biol.* **10** 75–82 PMID: 19197334
[55] Fletcher D A and Mullins R D 2010 Cell mechanics and the cytoskeleton *Nature* **463** 485–92
[56] Yarmola E G, Somasundaram T, Boring T A, Spector I and Bubb M R 2000 Actin-latrunculin a structure and function *J. Biol. Chem.* **275** 28120–7 PMID: 10859320
[57] Chalut K J, Höpfler M, Lautenschläger F, Boyde L, Chan C J, Ekpenyong A, Martinez-Arias A and Guck J 2012 Chromatin decondensation and nuclear softening accompany nanog downregulation in embryonic stem cells *Biophys. J.* **103** 2060–70
[58] Roti J L R, Kampinga H H, Malyapa R S, Wright W D, Van der Waal R P and Xu M 1998 Nuclear matrix as a target for hyperthermic killing of cancer cells *Cell Stress Chaperones* **3** 245–55 PMID: 9880237 PMCID: PMC312970
[59] Lepock J R 2004 Role of nuclear protein denaturation and aggregation in thermal radiosensitization *Int. J. Hyperthermia* **20** 115–30
[60] Mazumder A, Roopa T, Basu A, Mahadevan L and Shivashankar G V 2008 Dynamics of chromatin decondensation reveals the structural integrity of a mechanically prestressed nucleus *Biophys. J.* **95** 3028–35
[61] Redon C, Pilch D, Rogakou E, Sedelnikova O, Newrock K and Bonner W 2002 Histone H2A variants H2AX and H2AZ *Curr. Opin. Genet. Devel.* **12** 162–9 PMID: 11893489
[62] Dechat T, Pfleghaar K, Sengupta K, Shimi T, Shumaker D K, Solimando L and Goldman R D 2008 Nuclear lamins: major factors in the structural organization and function of the nucleus and chromatin *Genes Devel.* **22** 832 –853
[63] Hendzel M J, Boisvert F and Bazett-Jones D P 1999 Direct visualization of a protein nuclear architecture *Mol. Biol. Cell* **10** 2051–62 PMID: 10359614 PMCID: PMC25413

[64] Lepock J R, Frey H E, Heynen M L, Senisterra G A and Warters R L 2001 The nuclear matrix is a thermolabile cellular structure *Cell Stress Chaperones* **6** 136–47 PMID: 11599575 PMCID: PMC434391

[65] Uchida N, Kato H and Ishida T 1993 A model for cell killing by continuous heating *Med. Hypotheses* **41** 548–53 PMID: 8183133

[66] Bocklitz T, Putsche M, Stüber C, Käs J, Niendorf A, Rösch P and Popp J 2009 A comprehensive study of classification methods for medical diagnosis *J. Raman Spectrosc.* **40** 1759–65